ARTICLE

BIOTECHNOLOGY and BIOENGINEERING

An Actively Mixed Mini-Bioreactor for Protein Production From Suspended Animal Cells

Jinpian Diao,[1] Lincoln Young,[2] Peng Zhou,[2] Michael Louis Shuler[3,4]

[1]Genentech, Inc., 1 DNA Way, South San Francisco, California 94080

[2]Kionix, Inc., 36 Thornwood Drive, Ithaca, New York 14850

[3]School of Chemical and Biomolecular Engineering, Cornell University, Ithaca, New York 14853; telephone: 607-255-7577; fax: 607-255-1136; e-mail: mls50@cornell.edu

[4]Department of Biomedical Engineering, Cornell University, Ithaca, New York 14853

Received 10 June 2007; revision received 27 October 2007; accepted 7 November 2007

Published online 13 December 2007 in Wiley InterScience (www.interscience.wiley.com). DOI 10.1002/bit.21751

ABSTRACT: Biopharmaceutical production would benefit from rapid methods to optimize production of therapeutic proteins by screening host cell line/vector combination, culture media, and operational parameters such as timing of induction. Miniaturized bioreactors are an emerging research area aiming at improving the development speed. In this work, a 3 mm thick mini-bioreactor including two 12 mm wide culture chambers connected by a 5 mm wide channel is described. Active mixing is achieved by pressure shuttling between the two chambers. Gas-liquid phase exchange for oxygen and carbon dioxide is realized by molecular diffusion through 50 μm thick polymethylpentene membranes. With this unique design, a velocity difference between the middle area and the side areas at the interfaces of the culture chambers and the connecting channel is created, which enhances the mixing efficiency. The observed mixing time is on the order of 100 s. The combination of high permeability toward oxygen of polymethylpentene membranes and fluid movement during active pressure shuttling enables higher volumetric oxygen transfer coefficients, 5.7 ± 0.4–$14.8 \pm 0.6\ h^{-1}$, to be obtained in the mini-bioreactors than the values found in traditional 50 mL spinner flasks, 2.0–2.5 h^{-1}. Meanwhile, the calculated volume averaged shear stress, in the range of 10^{-2}–10^{-1} N/m^2, is within the typical tolerable range of animal cells. To demonstrate the applicability of this mini-bioreactor to culture suspended animal cells, the insect cell, *Spodoptera frugiperda*, is cultured in mini-bioreactors operated under a K_La value of $14.8 \pm 0.6\ h^{-1}$ and compared to the same cells cultured in 50 mL spinner flasks operated under a K_La value of 2.2 h^{-1}. Sf-21 cells cultured in the mini-bioreactors present comparable length of lag phases and growth rates to their counterparts cultured in 50 mL spinner flasks, but achieve a higher maximum cell density of $5.3 \pm 0.9 \times 10^6$ cell/mL than the value of $3.4 \pm 0.4 \times 10^6$ cell/mL obtained by cells cultured in 50 mL spinner flasks. Sf-21 cells infected with SEAP-baculovirus produce a maximum SEAP concentration of 11.3 ± 0.7 U/mL when cultured in the mini-bioreactor. In contrast, infected Sf-21 cells cultured in 50 mL spinner flasks produce a maximum SEAP concentration of 7.4 ± 0.9 U/mL and onset of production is delayed from 18 h in minibioreactor to 40 h in spinner flasks. Biotechnol. Bioeng. 2008;100: 72–81.

KEYWORDS: animal cell culture; microbioreactor; protein production

Correspondence to: M.L. Shuler

Background and Introduction

In modern biotechnology industries, cell culture plays a critical role enabling the large-scale production of biological products (Chu and Robinson, 2001; Flickinger and Drew, 1999; Shuler and Kargi, 2002). Due to the inherent complexity of animal cells, cellular physiological responses are very sensitive to the local culture environment. The number of genetic and process permutations needed to screen for new products and to allow process optimization is large; this drives a strong demand for obtaining accurate bioprocess data over a short time-frame. Additionally, the explosive recent development of high-throughput tools obtaining information at genomic and proteomic level (Henzel et al., 1993; Humphery-Smith et al., 1997; Klose and Kobalz, 1995; Schena et al., 1995; Yates et al., 1993) leaves information collection at cellular level the rate-limiting step in bioprocess development. What is required is the ability to perform a large number of cell culturing experiments under controlled environments in parallel with the capability of monitoring critical parameters in real-time. Such a capability would open a new avenue to the development of improved bioprocesses and a deeper understanding of the underlying biology.

Cell culture tools, such as T-flasks, microtiter plates, shake flasks, spinner flasks and 1–10 L bioreactors, have remained the standard bench-scale cell cultivation choices for decades

(Kumar et al., 2004; Stanbury et al., 1995). Extensive knowledge of these bioreactors and techniques of monitoring and controlling them have been established. However, considerable effort is required for pre-culture preparation and post-culture cleaning. As the number of experiments increases, the effort involved also scale up and quickly exceeds the handling capacity of individual experimentalists. Integrating steps that precede and follow cell cultivation with conventional bench-scale bioreactors would require building sophisticated mechanical systems. The complexity of these systems makes them expensive and fragile. Alternative technology to provide high-throughput, low cost, well controlled, robust and automated processing is clearly needed. Micro-bioreactor technology has been proposed as a potential solution to the deficiencies of existing bench-scale cell cultivation technology (Kostov et al., 2001; Lamping et al., 2003; Maharbiz et al., 2003; Zanzotto et al., 2004).

Micro-bioreactor technology is essentially a group of techniques including fabricating, operating, monitoring and controlling bioreactors at the scale of microliters to milliliters using parallel structures. Several micro-bioreactor designs have been proposed and tested for bioprocess development applications. Kostov et al. (2001) first adapted a 4 mL disposable polystyrene cuvette with a cross-sectional dimensions of 1 cm $\times$ 1 cm into a micro-bioreactor with a working volume of 2 mL. Oxygenation was achieved by placing a micro-sparger in the reactor, while mixing was realized by the action of a magnetic stirrer placed at the bottom of the well. Initial data on the responses of pH, dissolved oxygen and optical density using *Escherichia coli* as a model system demonstrated that fermentation in this micro-bioreactor was feasible. Lamping et al. (2003) machined a cylindrical micro-bioreactor from plexiglas with a diameter of 16 mm, a height of 48 mm and a working volume of 6 mL. A three, 6-bladed, open flat-turbine impeller was used to mix the medium, and an air sparger was placed directly beneath the hub of the bottom impeller. Using a Van't Riet analysis, Lamping et al. demonstrated that the oxygen transfer of their micro-bioreactor matched standard 20 L bioreactors. *E. coli* cultured in this type of micro-bioreactors showed comparable growth curves to *E. coli* cultured in 20 L fermenters operated under the same K_La value. Maharbiz et al. (2003) fabricated 250 μL microbioreactors out of plastic microplates connected to electrolysis chambers via 30 μm thick silicone membranes. Oxygen and carbon dioxide generated electrochemically in the electrolysis chambers penetrated through the silicone membranes into the culture chambers. Small steel beads were loaded into each culture chamber for stirring. Zanzotto et al. (2004) fabricated 5–50 μL chip-shaped micro-bioreactors (depth 300 μm) from poly (dimethylsiloxane) (PDMS) and covered them with a 100 μm thick oxygen-permeable PDMS membrane. The oxygen supply was realized by molecular diffusion from the gas phase to the liquid phase, and a K_La value up to 60 h^{-1} was obtained. Using *E. coli* as a model system, they presented dynamic curves for cell density, dissolved oxygen, pH, glucose, acetate, formate, and lactate that were similar to those observed in a 500 mL standard bioreactor operated under identical K_La values. Szita et al. (2005) and Zhang et al. (2005) improved Zanzotto's design by incorporating mini-magnetic stir bars into 150 μL chip-shaped PDMS micro-bioreactors (diameter 10 mm, depth 1 mm) for active mixing. The obtained K_La value was improved from $\sim$20 h^{-1} to $\sim$90 h^{-1} by increasing the rotation speed of the mini-magnetic stir bar from $\sim$200 rpm to $\sim$850 rpm. The dynamic cell growth curve and dissolved oxygen curve of two model systems, *E. coli* and *S. cerevisiae* were both improved as the value of K_La increased. Zhang et al. (2006) further incorporated a pressure-driven flow injection unit into the improved design and built a chemostat. Steady states of *E. coli* at different dilution rates were demonstrated. Following the similar chip-shape PDMS design, Lee et al. (2006) developed an integrated 100 μL micro-bioreactor arrays using embedded air actuation micro-channels for mixing and oxygenating simultaneously. The obtained K_La value was improved as mixing efficiency increased with a maximum K_La of 360 h^{-1}. *E. coli* cultured in these micro-bioreactors presented maximum cell density comparable to a reference 4 L fermentation. Separately, Rao et al. pioneered the application of optical chemical sensing technology to monitor primary operational parameters including pH, dissolved oxygen and carbon dioxide (Ge et al., 2003, 2005; Kostov et al., 2001).

As reviewed above, existing mini-bioreactor prototypes have successfully demonstrated the feasibility of culturing and monitoring cells at micro-scale. However, their applications have focused on bacterial and yeast fermentation. Yet, animal cell cultivation plays an important role in modern bioprocess engineering due, for example, to their unique capability of adding complex glycans (Flickinger and Drew, 1999; Mohamed, 2002; Shuler and Kargi, 2002). Animal cells are notorious for their susceptibility to hydrodynamic stress due to the lack of cell walls. Published documents indicate that a shear stress above 1 N/m^2 is lethal to most animal cells and results in cell lysis (Ma et al., 2002). Moderate level of shear stress below 1 N/m^2 could trigger non-lethal, yet physiologically significant, changes in cells (Ma et al., 2002; Shuler et al., 1995). Thus controlling hydrodynamic forces within the tolerance of cell lines typically used in bioprocessing is a critical concern for bioreactor design. Animal cells are also very sensitive to osmotic pressure and evaporation of fluid during cell culture can be highly detrimental. Gas transfer must selectively favor oxygen and carbon dioxide while minimizing water evaporation.

In this work, a mini-bioreactor for culturing suspended animal cells was designed and fabricated from polyacrylic acid with a polymethylpentene membrane. This new design contained two elongated chambers connected by a channel with significantly reduced cross-sectional dimension as shown in Figure 1. The elongated chambers were enclosed by polymethylpentene membranes to facilitate oxygen and CO_2 exchange through molecular diffusion. These membranes have low permeability for water vapor. Mixing was achieved

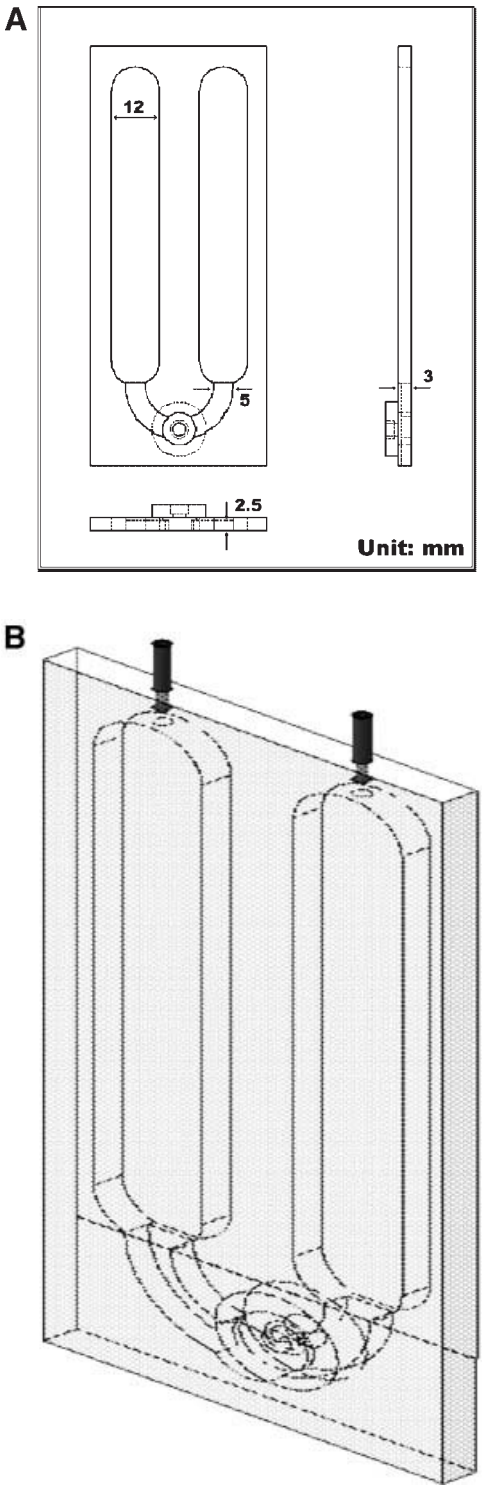

Figure 1. Schematic diagrams of the mini-bioreactor. **A**: Anatomic 3D drawings of the middle frame. The middle frame is composed of two vertical cut-through openings, 12 mm wide, connected by a narrow U-channel, 5 mm wide and 2.5 mm deep. The whole structure is 3 mm thick. A hole is opened at the bottom of the U-channel for inserting of a micro oxygen probe. **B**: A 3D drawing of the assembled mini-bioreactor. The two sides of the middle frame are covered by 50 μm thick polymethylpentene membranes. Two holes are drilled through the top of the mini-bioreactor and embedded with tubes to be connected with external tubing and filters. These holes are used to seed cell culture, remove samples and control the internal pressure.

by continuously shuttling the culture medium between two chambers using an oscillatory regulating pressure. Shear stress within this novel mini-bioreactor was approximated using a numerical model. The mixing time and K_La of this mini-bioreactor were also characterized under different operational conditions. An insect Sf-21 cell line was used as a model system to demonstrate the feasibility of this novel mini-bioreactor for culturing suspended animal cells. Cell growth and protein expression curves were compared with those obtained from standard 50 mL spinner flasks.

Materials and Methods

Design, Fabrication, and Sterilization

The mini-bioreactor adopted a chip design. A pattern of two parallel 12 mm wide channels connected by a 5 mm wide U-channel was cut onto 3 mm thick polyacrylic acid sheets as shown in Figure 1A. A hole was drilled through the middle of the U-channel to plug into a micro oxygen probe. Holes were also drilled through the top of each 12 mm wide channel and nickel tubes were chiseled in as gas outlets. The two sides of the frame were covered by 50 μm thick polymethylpentene membranes. Assembled mini-bioreactors are shown in Figure 1B.

Layouts of the mini-bioreactors were drawn by Solid Works (SolidWorks Co., Concord, MA) and milled onto polyacrylic acid sheets (Cryo Industries, Chicago, IL) locally by Kionix, Inc. (Ithaca, NY) using a standard mill machine (OM2A, Haas Automation, Inc., Oxnard, CA). Fifty microliters thick double-side adhesive sheets (ARclad® 7876, Adhesives Research, Inc., Glen Rock, PA) were then attached to both sides of the polyacrylic frame. The middle of the attached adhesive sheets was removed along the pattern of the milled frame using razors. Fifty microliters thick polymethylpentene sheets (Curbell, Orchard Park, NY) were attached to the exposed side of the adhesive sheets.

Assembled mini-bioreactors were sterilized by a standard ethylene dioxide sterilization procedure. During cell culture, the medium was loaded into mini-bioreactors using syringes and needles in a sterilized laminar flow hood. Syringes were overfilled with liquid medium to avoid injecting air into the mini-bioreactors. Autoclaved 0.2 μm filters (Sterile Syringe Filter, w/0.2 μm cellulose acetate membrane, VWR, West Chester, PA) were connected to the two gas outlets through autoclaved tubing to prevent contamination.

Device Operation

During operation, assembled mini-bioreactors loaded with cell culture were placed in a humid carbon dioxide incubator which maintained constant temperature and humidity. Figure 2 shows a schematic description of the whole configuration. 2.5 mL of cell culture was loaded into each assembled mini-bioreactor, which was placed upright on

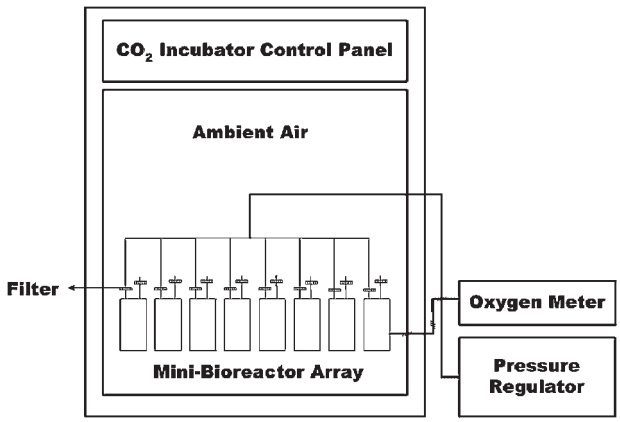

Figure 2. Schematic description of the configuration of the cell culturing system. Multiple mini-bioreactors are placed in a CO_2 incubator maintaining constant temperature. One outlet tube on top of each mini-bioreactor is connected with tubing linked to an external pressure regulator regulating pressure. Micro oxygen probes and accompanying oxygen meters are used to monitor dissolved oxygen.

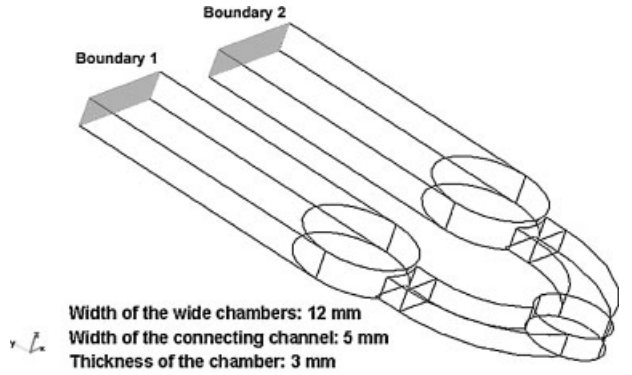

Figure 3. A schematic drawing of the numerical model. The dimensions of the numerical model are the same as the physical model shown in Figure 1. The inflow velocity at Boundary 1 was set equal to the experimentally measured moving velocity of the air–water interface. Boundary 2 was set as outflow.

holders. The two outlets at the top were connected to a pressure regulator and ambient pressure via air filters and tubing, respectively. At the beginning, the liquid–air interfaces in the two parallel chambers were at the same level. Once the pressure regulator were turned on, the pressure in the headspace of the chamber connected to the pressure regulator was regulated between a pre-set pressure and a vacuum at a specified frequency. Liquid in the mini-bioreactor was pushed by the net force of the pressure differential and gravity force until the pressure differential was equal to the gravity force. In this way, the pressure differential between the two parallel chambers drove the liquid in the mini-bioreactor to move back and forth periodically.

Shear Stress Characterization

The shear stress generated in the mini-bioreactor was calculated based on incompressible Navier-Stokes equations using Femlab (Femlab version 3.1, Comsol, Burlinton, MA) for the conditions considered in the experimental study. In the present study, the numerical model was built with the same dimensions as the physical model shown in Figure 3. The reactor was filled with water at 20°C. The moving velocity of the air–water interface was obtained experimentally and used to define the boundary condition of the air–water interface under the control of the external pressure regulator. The boundary condition of the other air–water interface where the chamber was connected to the ambient pressure was set as outflow. The experimental procedure of obtaining the moving velocity of the air–water interface is described in the next paragraph.

The moving velocity of the air–water interface was obtained by dividing the moving distance of the interface over the time under the regulating pressure. The moving distance of the interface was monitored by eye using a ruler. The time was recorded using a stopwatch.

Mixing Time Characterization

The mixing capability of the new mini-bioreactor was quantified using a conventional colorimetric method for determining mixing time based on acid–base reactions (Paul et al., 2004). In this method, mixing time was defined as the time required to observe a color change from pink to clear during an acid-base neutralization reaction. Fifty microliters of a 0.1 M NaOH solution and 50 μL of a 1% phenolphthalein solution were mixed and diluted into 50 mL of distilled water. A certain volume of the pre-mixed base solution specified in each experiment was added to the mini-bioreactors. At time zero, 0.1 M HCl solution with a volume of 1% of pre-loaded base solution was injected into the bioreactor quickly using a 200 μL pipetman. The disappearance of the pink color was observed by eye, and the time was recorded using a stopwatch. The pipetman was always placed at the same position in the micro-bioreactor in all of the experiments undertaken here.

K_La Characterization

The "unsteady" method (Shuler and Kargi, 2002) was used to evaluate the K_La value obtained in 3 mm thick mini-bioreactors filled with Ex-Cell 400 serum-free medium (JRH Biosciences, Lenexa, KS). During measurement, a mini-bioreactor was placed in a closed chamber within an incubator. The chamber has specific openings for delivery of desired gas mixtures and ports for the exhaust of gas. Tubing delivering nitrogen and air were attached to this chamber.

A micro-oxygen probe (MI-730 Oxygen Electrode, Microelectrodes, Inc., Bedford, NH) was inserted into the reactor. At beginning, the chamber was flushed with nitrogen until the residual dissolved oxygen (DO) in the medium was zero. Subsequently, the nitrogen flow was turned off and an air flow was pumped into the chamber. The DO recovery was recorded by a micro-oxygen probe. The K_La values were obtained from the following expression:

$$K_La = -\frac{\ln(C^* - C_{t_2}) - \ln(C^* - C_{t_1})}{t_2 - t_1} \quad (1)$$

where t is time (h), C is the DO concentration in the liquid phase (mg/L), and C^* is the saturated DO concentration (mg/L).

Insect Sf-21 Culture Medium and Maintenance

Spodoptera frugiperda (IPL-Sf21AE) cells were obtained from Dr. Robert Granados at the Boyce Thompson Institute for Plant Research (Ithaca, NY). The Sf-21 cells were adapted to Ex-Cell 400 serum-free medium from a TNM-FH medium (containing 10% Fetal Bovine Serum) in a suspension culture. Adaptation was accomplished by slowly weaning the cells from the serum-containing medium. The Sf-21 cells were grown at 28°C in a suspension culture using 50 mL spinner flasks (Bellco Glass, Vineland, NJ) with a working volume of 40 mL agitated at 100 rpm. The normal caps were replaced with foam closures (Bellco Glass) to facilitate better oxygen transfer. Frozen cells were revived and maintained in 25 mL T-flasks for three passages, then transferred to 50 mL spinner flasks and maintained for at least three passages before they were used in any spinner flask and mini-bioreactor experiments. Cells were routinely subcultured every 2–3 days.

SEAP Baculovirus Stock Preparation and Titer Measurement

Baculovirus containing the gene for secreted alkaline phosphatase (SEAP) was produced using the 1A strain of *Autographa californica* nucleopolyhedrovirus (AcMNPV) and a secreted form of the gene for human placental alkaline phosphatase in the pAc YM1 vector and was obtained from Dr. Alan Wood at the Boyce Thompson Institute for Plant Research. Virus was amplified by infecting actively growing Sf-21 cells at 2×10^6 cells/mL (corresponding to a mid-exponential phase) at a multiplicity of infection (MOI) of two. A low MOI reduced the production of defective interfering particles. The virus was harvested 2 days post infection.

The virus was titrated using a modified end-point dilution assay (Dee and Shuler, 1997). For the modified end-point dilution assay, each well of a 96-well-plate was seeded with 50 μL of Sf-21 broth. Ten microliters of diluted virus was added per well and the plate was spun at 1,000*g* for 1 h in a centrifuge (Allegra™ X-12 Centrifuge, Beckman Coulter, Fullerton, CA). After incubation at 28°C for 7 days, 25 μL of 1 mg/mL 5-bromo-4-chloro-3-indolyl phosphate (BCIP) (Sigma, St. Louis, MO) were added to each well. The proportion of wells that turned blue was determined 4–6 h after the addition of the substrate.

Insect Sf-21 Cell Growth Experiments

Cells were maintained in spinner flasks and used when they reached a density of about $2–3 \times 10^6$ cells/mL (corresponding to a mid-exponential phase) with a viability >95%. For the mini-bioreactor experiments, Sf-21 cells were seeded at 5×10^5 cells/mL into mini-bioreactors shuttled under a pressure differential of 548.0 Pa and a shuttling frequency of 2.14 Hz with a working volume of 2.5 mL. The cell number was determined every 24 h using a hemocytometer (Brialit Live™, Reichert, Buffalo, NY). Cell viabilities were measured using trypan blue dye exclusion. For spinner flasks, Sf-21 cells were seeded into spinner flasks agitated at 100 rpm. with a working volume of 40 mL at 5×10^5 cells/mL. Cell numbers and viability were determined in the same way for the mini-bioreactors. The results presented here involved an average of three replicate devices at each time point.

Insect Sf-21 Infection Experiments

Cells were maintained in spinner flasks. When the cells had reached $2–3 \times 10^6$ cells/mL with a viability of >95% (corresponding to a mid-exponential phase), the cells were harvested by centrifugation at 100*g* for 10 min in a centrifuge (Allegra™ X-12 Centrifuge, Beckman Coulter), pooled and resuspended in fresh medium at $5–6 \times 10^6$ viable cells/mL in spinner flasks. Virus was added to give a MOI of 10. Cells were incubated with the virus for 3.5 h in spinner flasks agitated at 100 rpm. The cells were then centrifuged and resuspended at 3×10^6 cells/mL in fresh medium in both mini-bioreactors and spinner flasks. SEAP expression was quantified by the SEAP assay every 24 h post placement in the reactors.

Secreted Alkaline Phosphatase Determination

Extracellular SEAP activity was measured every 24 h up to a total time of 7 days. A 0.1 mL aliquot of medium was removed from bioreactors and centrifuged to pellet the cells (Allegra™ X-12 Centrifuge, Beckman Coulter). The sample was heated at 65°C for 5 min to eliminate endogenous phosphatase activity and then microcentrifuged for 2 min (Micro-Centrifuge Model 235C, Fisher Scientific, Hampton, NH). Five microliters of sample was added to 1 mL of assay buffer (1.0 M diethanolamine pH 9.8, 0.5 mM $MgCl_2$ and 10 mM L-homoarginine) (Sigma) and 100 μL of 120 mM p-nitrophenyl phosphate (Sigma) (in assay buffer) and

allowed to incubate at 28°C. The absorbance at 405 nm was monitored for 45 s. The slope was used to calculate the SEAP activity.

Results and Discussion

Shear Stress Characterization

Extensive previous work (Ma et al., 2002; McQueen et al., 1987; Shuler et al., 1995) shows that shear stress has significant impact on animal cells' performance. A modest level of shear stress is important to emulate shear-induced physiological changes in a scale-up reactor and static cultures might not provide good prediction of performance under shear. However, high levels of shear stress, >1 N/m^2, will also be detrimental to most animal cells. Figure 4 shows the volume-average shear stress corresponding to the shuttling speed generated in a 3 mm thick mini-bioreactor calculated using Femlab. It can be seen that, within the tested range of shuttling speed, 0.1–2 cm/s, the volume-average shear stress is well below the typical lethal threshold value for suspended animal cells, 1 N/m^2 (Ma et al., 2002; Shuler et al., 1995). Figure 5 shows the detailed shear stress profiles in the *x*, *y*, *z* directions when a 3 mm thick mini-bioreactor is shuttled under 1 cm/s. The shear stress mainly occurs in the narrow connecting channel and the interface between the connecting channel and the vertical chamber. The maximum shear stress is 0.18 N/m^2, which is also far below the typical lethal threshold value for suspended animal cells, 1 N/m^2. Collectively, these approximate estimations suggest that the shear stress generated in the 3 mm thick mini-bioreactor will not be severe enough to cause significant death of animal cells. Yet, it may have physiologically relevant effects on the cultured cells.

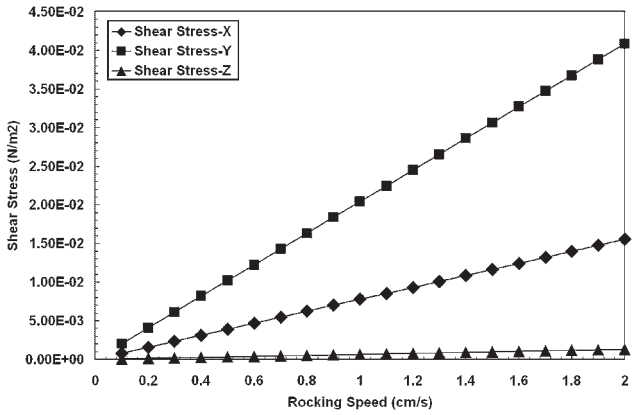

Figure 4. The volume-average shear stress generated in a 3 mm thick mini-bioreactor corresponding to the shuttling speed.

Mixing Time Characterization

Figure 6 shows the mixing times for a 3 mm thick mini-bioreactor shuttled under different conditions and various working volumes. The mixing time ranges between 12 and 120 s when 3 mm thick mini-bioreactors are operated with a 1.5–2.5 mL working volume, a pressure differential of 174.4–548.0 Pa and a 5.00–2.14 Hz shuttling frequency. The influence of regulating pressure to the mixing time is nonlinear: the mixing time increases to a larger extent at low regulating pressure regions and large working volume, but to a smaller extent at high regulating pressure regions and low working volume. Shuttling frequency, in general, has less influence on the mixing time than the values of the regulating pressure and working volume within the tested range. Comparing the measured mixing time range to the typical time scales of substrate consumption (5.5×10^4 s), cell growth (1.2×10^4 s), and heat production (350 s) (Shuler and Kargi, 2002) for large scale reactors, it can be seen that the mixing time scale generated in a 3 mm thick mini-bioreactor is much shorter than these kinetic time scales. It is concluded that the above three reactions are kinetically limited rather than transport limited and there should be little or no cell density and glucose concentration heterogeneity and heat accumulation.

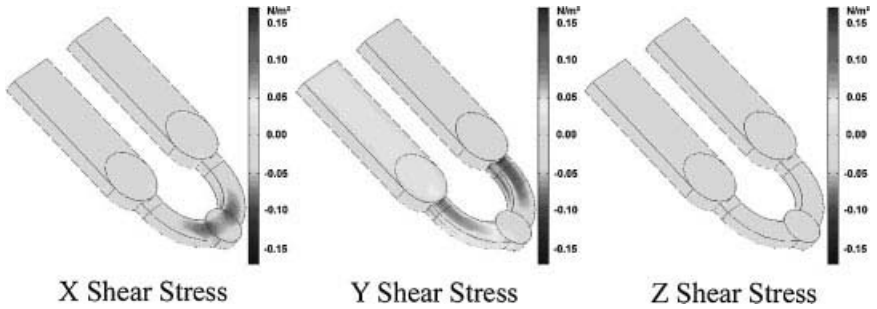

Figure 5. The shear stress profiles in the *x*, *y*, *z* directions generated in a 3 mm thick mini-bioreactor shuttled at 1 cm/s.

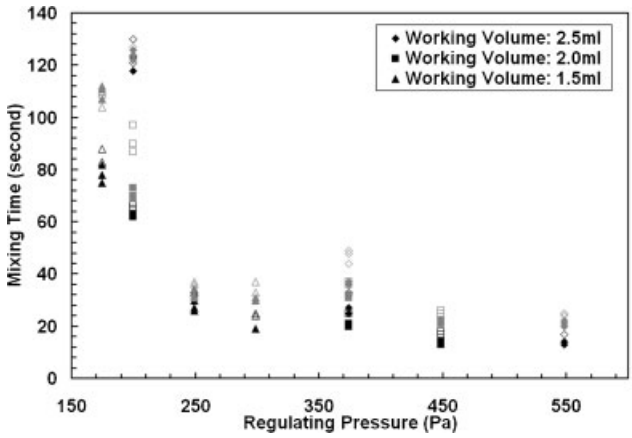

Figure 6. Mixing time obtained in a 3 mm thick mini-bioreactor operated under various conditions. (◆) Working volume 2.5 mL and shuttling frequency 5 Hz; (■) Working volume 2.0 mL and shuttling frequency 5 Hz; (▲) Working volume 1.5 mL and shuttling frequency 5 Hz; (◇) Working volume 2.5 mL and shuttling frequency 3.75 Hz; (□) Working volume 2.0 mL and shuttling frequency 3.75 Hz; (Δ) Working volume 1.5 mL and shuttling frequency 3.75 Hz; (◈) Working volume 2.5 mL and shuttling frequency 3 Hz; (▩) Working volume 2.0 mL and shuttling frequency 3 Hz; (◭) Working volume 1.5 mL and shuttling frequency 3 Hz; (◇) Working volume 2.5 mL and shuttling frequency 2.5 Hz; (▣) Working volume 2.0 mL and shuttling frequency 2.5 Hz; (△) Working volume 1.5 mL and shuttling frequency 2.5 Hz.

Oxygen Transportation Characterization

In the present design, oxygen transfer is mainly achieved by diffusion through the polymethylpentene membranes covering two sides of the mini-bioreactors. Polymethylpentene has selectively large permeabilities of oxygen and carbon dioxide and a low permeability of water vapor (Brandrup and Immergut, 1975). Figure 7 presents the volumetric oxygen transfer coefficients, K_La, of a 3 mm thick mini-bioreactor covered by 50 μm thick polymethylpentene membranes operated under various regulating pressures and shuttling frequencies. The ranges of these values lie between 5.7 ± 0.4 and 14.8 ± 0.6 h^{-1} as the regulating pressure and shuttling frequency increase. These values are larger than reported K_La values for 50 mL spinner flasks filled with 40 mL of the same culture medium operated between 60 and 100 rpm, which have been found to be between 2.0 and 2.5 h^{-1} (Taticek, 1995). Additionally, it is notable that there is a large increase of K_La values as the regulating pressure increases from a pressure differential of 199.3 Pa to a pressure differential of 373.7 Pa, while there is no significant increase of K_La values as the regulating pressure increases from a pressure differential of 373.7 Pa to a pressure differential of 548.0 Pa.

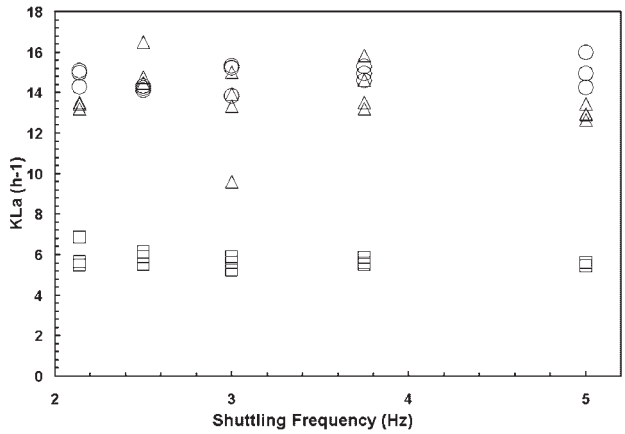

Figure 7. Volumetric oxygen transfer coefficients, K_La, of a 3 mm thick mini-bioreactor operated under various conditions. (□) Shuttling pressure 199.3 Pa; (Δ) Shuttling pressure 373.7 Pa; (○) Shuttling pressure 548.0 Pa.

The plateau of K_La at high regulating pressure can be explained by the fact that the oxygen supply from the air to the culture medium is realized by the oxygen diffusion from the air to culture medium through the polymethylpentene membrane. Therefore, the overall oxygen mass-transfer resistance, $1/k_{total}$, is the sum of the oxygen diffusion resistance through the polymethylpentene membrane, $1/k_{membrane}$, the oxygen mass-transfer resistance in the culture medium, $1/k_C$, and the oxygen mass-transfer resistance in the gas phase, $1/k_g$, as shown in Equation (2) (Cussler, 1997):

$$\frac{1}{k_{total}} = \frac{1}{k_g} + \frac{1}{k_{membrane}} + \frac{1}{k_C} \tag{2}$$

and the $1/k_{membrane}$ can be derived from Equation (3) (Cussler, 1997):

$$\frac{1}{k_{membrane}} = \frac{t}{D_{polymethylpentene}H} \tag{3}$$

where t is the thickness of the membrane (μm), D is the diffusivity of oxygen in polymethylpentene (cm^2/s), and the Henry's constant H, is the solubility ratio of oxygen in polymethylpentene and water. Increase of regulating pressure enhances the mixing and distribution of dissolved oxygen in the culture medium, therefore, reduces the oxygen mass-transfer resistance in the culture medium, $1/k_C$, and the overall oxygen mass-transfer resistance, $1/k_{total}$. Because the oxygen–liquid interfacial area (cm^2/cm^3), a, stays constant during the operation of the mini-bioreactor, the above results further lead to increased K_La, which is the multiple of k_{total} and a. The plateau of the K_La at high regulating pressure suggests that the $1/k_C$ has reached its minimum. Any further reduction in $1/k_{total}$, depends on reducing the values of $1/k_{membrane}$ and $1/k_g$.

To further understand the significance of the contribution of the $1/k_{membrane}$ and $1/k_g$ to $1/k_{total}$, the minimum $1/k_{total}$ that can be obtained in the 3 mm thick 3 mL mini-bioreactor covered with 50 μm thick polymethylpentene membranes was calculated as 1,313 s/cm, given that the maximum K_La obtained experimentally is, 14.2 ± 1.3 h^{-1}, and the a, determined by the present design, is 5.2 cm^2/cm^3. Additionally, using Equation (3) and the values of

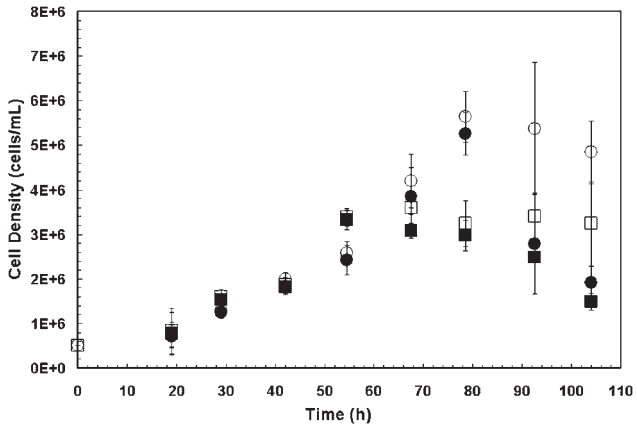

Figure 8. Cell growth curves of Sf-21 cultured in 50 mL spinner flasks and 3 mL mini-bioreactors. (○) Total cell density obtained in 3 mL mini-bioreactor (3 mm thick, 2.5 mL working volume, 548.0 Pa regulating pressure and 2.14 Hz shuttling frequency); (●) Viable cell density obtained in 3 mL mini-bioreactor; (□) Total cell density obtained in 50 mL spinner flask (40 mL working volume and 100 rpm agitation speed); (■) Viable cell density obtained in 50 mL spinner flask. The results are the average of three replicates.

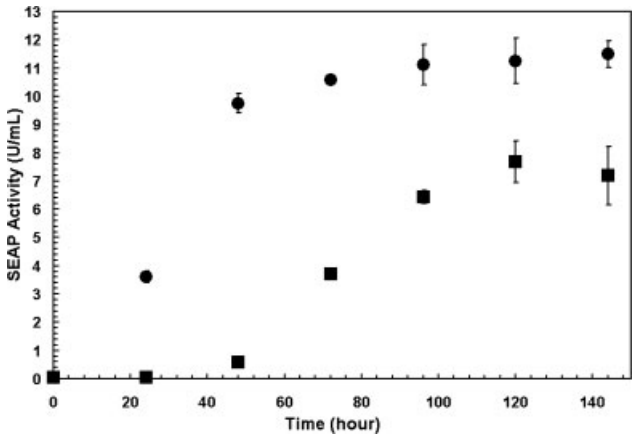

Figure 9. Time curves of SEAP expression and secretion by SEAP-baculovirus infected Sf-21 cultured in Ex-400 medium. (●) Infected Sf-21 cultured in 3 mL mini-bioreactors (3 mm thick, 2.5 mL working volume, 548.0 Pa regulating pressure and 2.14 Hz shuttling frequency); (■) Infected Sf-21 cultured in 50 mL spinner flasks (40 mL working volume and 100 rpm agitation speed). The results are the average of three replicates.

$S_{\text{polymethylpentene}}$ as 0.243 $\text{cm}^3(\text{STP})\,\text{cm}^{-3}\,\text{atm}^{-1}$ (Brandrup and Immergut, 1975), S_{water} as 7.36 $\text{mg}\,\text{L}^{-1}$ [1] (Perry and Green, 1984), and $D_{\text{polymethylpentene}}$ as 1.01×10^{-6} $\text{cm}^2\,\text{s}^{-1}$ (Brandrup and Immergut, 1975), the $1/k_{\text{membrane}}$ of 50 μm thick polymethylpentene membrane was calculated as 500 s/cm according to its definition. Compared with the $1/k_{\text{total}}$, it can be seen that the $1/k_{\text{membrane}}$ contributes about 38% of the $1/k_{\text{total}}$. This result suggests that designing a custom incubator for the mini-bioreactors to reduce $1/k_{\text{g}}$ would be equally important as trying alternative membranes with high oxygen diffusivity and solubility to obtain better overall oxygen supply. To mimic the response of larger scale bioreactors, it is unlikely that increased $K_{\text{L}}a$ will be needed.

Insect Sf-21 Growth and SEAP Production Kinetics

As a model cell-line, inset cell Sf-21 was cultured in mini-bioreactors and spinner flasks to compare the cell growth and recombinant protein production kinetics. Under the culture conditions specified in the method section, no bubbles were formed through the culture process. No significant cell attachment was observed until the end of culture. There was also no observable loss of liquid in the mini-bioreactor during the period of operation.

Figure 8 presents the growth curve of Sf-21 cultured in mini-bioreactors and in spinner flasks. Sf-21 cells grown in 3 mL 3 mm thick mini-bioreactors shuttled under a pressure differential of 548.0 Pa at 2.1 Hz exhibit high viability, approximately 100%, up to the middle-late exponential phase. The viability drops significantly thereafter. The length of lag phase, ~15 h, and specific growth rate, 0.035 h^{-1}, are essentially the same as Sf-21 cells grown in 50 mL spinner flasks agitate at 100 rpm. Previous work (Taticek et al., 2001) has shown that 100 rpm was an optimal agitation speed to obtain high specific growth rate of Sf-21 cultured in 50 mL spinner flasks and reported a similar specific growth rate of 0.034 h^{-1}. However, cells grown in mini-bioreactors reach a higher total density of $5.3 \pm 0.9 \times 10^6$ cell/mL at the stationary phase than cells grown in spinner flasks with the maximum cell density of $3.4 \pm 0.4 \times 10^6$ cell/mL. Figure 9 presents the SEAP production kinetics of Sf-21 after infection by SEAP-baculovirus. Infected Sf-21 cells cultured in 3 mL 3 mm thick mini-bioreactors shuttled under a pressure differential of 548.0 Pa at 2.1 Hz show an 18 h long lag phase, with a maximum secreted SEAP concentration at about 72 h post-infection. The obtained maximum SEAP concentration is about 11.3 ± 0.7 U/mL in the mini-bioreactor. In contrast, infected Sf-21 cells cultured in 50 mL spinner flasks and agitated at 100 rpm show a significant lag phase of, ~40 h, and reach a maximum SEAP concentration at about 120 h post-infection. The maximum SEAP concentration is about 7.4 ± 0.9 U/mL.

The differences presented by Sf-21 cultured in mini-bioreactors and spinner flasks reflect critical design uniqueness of the mini-bioreactor. The comparable specific growth rate and higher maximal cell density achieved in mini-bioreactors in the cell growth stage indicates a more sustainable environment for cells to grow to higher extent. This could be from slower consumption of certain nutrients in the medium or slower accumulation of toxins. Whatever factors they may be, they must be the results of different

[1] In equilibrium with 0.21 atm oxygen.

cellular metabolism. In published databases, oxygen supply is repetitively discussed as a major engineering factor affecting cell performance. Insect cells are known for their high oxygen uptake rate (Maiorella et al., 1988; Weiss et al., 1982). When no other limiting factors exist, higher oxygen supply leads to faster growth and higher maximal cell density. Cells growing under oxygen deficiency produce an inhibitory factor, lactate, significantly (Bhatia et al., 1997). Under the culture conditions in this study, mini-bioreactors do have a higher K_La of 14.8 ± 0.6 h^{-1} than spinner flasks with a K_La of 2.5 h^{-1}. The higher K_La might also explain the earlier onset of SEAP production and higher maximal SEAP concentration in mini-bioreactors in the post-infection stage. Several separate studies indicate that the oxygen uptake rate increase dramatically soon after infection (Kamen et al., 1991; Maiorella et al., 1988; Reuveny et al., 1993; Schopf et al., 1990; Weiss et al., 1982). Earlier expression of recombinant proteins and higher protein concentration were observed under higher oxygen supply (Taticek and Shuler, 1997). Other than oxygen supply, shear stress is also indicated playing important roles on affecting the performance of insect cells cultured in reactors. Shear stress above 1 N/m^2 is reported leading to observed cell death (Tramper et al., 1986) while stress below this value might still trigger faster consumption of energy resources to repair the induced damage (Cowger et al., 1999). It follows that at converse, a reduction of shear stress would account for higher maximal cell density. This is also consistent with the shorter lag phase and higher SEAP expression rate obtained in mini-bioreactors, since it is known that the size of Sf-21 cells infected with baculovirus increases and they are more sensitive to shear stress than uninfected cells (Taticek, 1995). Unlike oxygen supply and shear stress whose effects are extensively studied, few reports exist on the effects of carbon dioxide accumulation in insect cells. Yet limited published data show that carbon dioxide accumulation did limit the cell growth and protein expression (Garnier et al., 1996; Mitchell-Logean and Murhammer, 1997). Collectively, the higher maximal cell density, earlier onset of protein expression and higher protein concentration achieved in mini-bioreactors all suggest a favorable environment in mini-bioreactors, that is, efficient oxygen supply, carbon dioxide removal and low shear stress. Certainly, more work needs to be done to systematically characterize this novel mini-bioreactor and understand it capability. Knowledge from these studies will enable future design improvement to optimize performance.

Conclusions

In the present work, a pressure-mixed and chip-shaped mini-bioreactor was developed. The application of pressure-mixing mechanism eliminates the need for a complicated fabrication process that incorporates an internal mechanical bar. The thin chip-design using a narrow channel connecting two wider chambers creates a velocity difference between the middle area and the side areas at the interfaces of the wide culture chambers and the connecting channel, enhancing the mixing efficiency. The mixing time obtained by this design is sufficiently short to minimize any mass transfer limitation. The usage of polymethylpentene membranes as the covering material enables high transportation of oxygen while minimizing water loss. Meanwhile the volume averaged shear stress is within the physiologically tolerable range for animal cells. Additionally, due to the simple nature of this design, simple standard milling techniques are sufficient to fabricate the desired structures. With its ability to use inexpensive plastic materials such as polyacrylic acid, the cost of fabrication is much lower than other processes which require sophisticated fabrication techniques.

Sf-21 cells cultured in mini-bioreactors exhibited comparable lag phases and growth rates, but a higher maximum cell density than cells cultured in 50 mL spinner flasks operated at a lower K_La. SEAP-baculovirus infected Sf-21 cells cultured in mini-bioreactors operated at a K_La value of 14.8 ± 0.6 h^{-1} exhibited an 18-h lag phase and a maximum SEAP concentration of 11.3 ± 0.7 U/mL. While, the values obtained by the same infected cells cultured in 50 mL spinner flasks operated at a K_La value of 2.5 h^{-1} showed a 40-h lag phase and a maximum SEAP concentration of 7.4 ± 0.9 U/mL. These initial data suggest that this thin polymethylpentene membrane-covered and pressure-shuttled mini-bioreactor provides a favorable environment to culture and study suspended animal cells producing proteins.

We thank NYSTAR and Cornell Center for Advanced Technology for their generous financial support of this project. Also, we are in debt to the scientists and engineers at Kionix, Inc., for their technical and financial contribution. Publication costs and continuing support from Pfizer is also acknowledged. We are thankful to Dr. Robert Granados in providing the *Spodoptera frugiperda* (IPL-Sf21AE) cells.

References

Bhatia R, Jesionowski G, Ferrance J, Ataai MM. 1997. Insect cell physiology. Cytotechnology 24:1–9.

Brandrup J, Immergut EH, editors. 1975. Polymer handbook. New York: John Wiley & Sons.

Chu L, Robinson DK. 2001. Industrial choices for protein production by large-scale cell culture. Curr Opin Biotechnol 12(2):180–187.

Cowger NJ, O'Connor KC, Hammond TG, Lacks DJ, Navar GL. 1999. Characterization of bimodal cell death of insect cells in a rotating-wall vessel and shaker flask. Biotechnol Bioeng 64:14–26.

Cussler EL. 1997. Diffusion: Mass transfer in fluid system. Cambridge: Cambridge university press.

Dee KU, Shuler ML. 1997. Optimization of an assay for baculovirus titer and design of regimens for the synchronous infection of insect cells. Biotechnol Prog 13(1):14–24.

Flickinger MC, Drew SW, editors. 1999. Encyclopedia of bioprocess technology—Fermentation, biocatalysis, and bioseparation. New York: John Wiley & Sons.

Garnier A, Voyer R, Tom R, Perret S, Jardin B, Kamen A. 1996. Dissolved carbon dioxide accumulation in a large scale and high density

production of TGFβ with baculovirus infected Sf-9 cells. Cytotechnology 22: 53–63.
Ge X, Kostov Y, Rao G. 2003. High-stability non-invasive autoclavable naked optical CO_2 sensor. Biosens Bioelectron 18(7):857–865.
Ge X, Kostov Y, Rao G. 2005. Low-cost non-invasive optical CO_2 sensing system for fermentation and cell culture. Biotechnol Bioeng 89(3): 329–334.
Henzel WJ, Billeci TM, Stults JT, Wong SC, Grimley C, Watanabe C. 1993. Identifying proteins from two-dimensional gels by molecular mass searching of peptide fragments in protein sequence databases. Proc Natl Acad Sci 90(11):5011–5015.
Humphery-Smith I, Cordwell SJ, Blackstock WP. 1997. Proteome research: Complementarity and limitations with respect to the RNA and DNA worlds. Electrophoresis 18(8):1217–1242.
Kamen AA, Thom RL, Caron AW, Chavarie C, Massie B, Archambault J. 1991. Culture of insect cells in a helical ribbon impeller bioreactor. Biotechnol Bioeng 38:619–628.
Klose J, Kobalz U. 1995. Two-dimensional electrophoresis of proteins: An updated protocol and implications for a functional analysis of the genome. Electrophoresis 16(6):1034–1059.
Kostov Y, Harms P, Randers-Eichhorn L, Rao G. 2001. Low-cost microbioreactor for high-throughput bioprocessing. Biotechnol Bioeng 72(3):346–352.
Kumar S, Wittmann C, Heinzle E. 2004. Minibioreactors. Biotechnol Lett 26(1):1–10.
Lamping SR, Zhang H, Allen B, Ayazi Shamlou P. 2003. Design of a prototype miniature bioreactor for high-throughput automated bioprocessing. Chem Eng Sci 58(3):747–758.
Lee HLT, Boccazzi P, Ram RJ, Sinskey AJ. 2006. Microbioreactor arrays with integrated mixers and fluid injectors for high throughput experimentation with pH and dissolved oxygen control. Lab on a Chip 6(9):1229–1235.
Ma NN, Koelling KW, Chalmers JJ. 2002. Fabrication and use of a transient contractional flow device to quantify the sensitivity of mammalian and insect cells to hydrodynamic forces. Biotechnol Bioeng 80(4):428–437.
Maharbiz MM, Holtz WJ, Howe RT, Keasling JD. 2003. Microbioreactor arrays with parametric control for high-throughput experimentation. Biotechnol Bioeng 85(4):376–381.
Maiorella B, Inlow D, Shauger A, Harano D. 1988. Large-scale insect cell-culture for recombinant protein production. Bio/Technology 6:1406–1410.
McQueen A, Meilhoc E, Bailey J. 1987. Flow effects on the viability and lysis of suspended mammalian cells. Biotechnol Lett 9:831–836.
Mitchell-Logean C, Murhammer DW. 1997. Bioreactor headspace purging reduces dissolved carbon dioxide accumulation in insect cell cultures and enhances cell growth. Biotechnol Prog 13:875–877.
Mohamed A-R, editor. 2002. Glycosylation. Dordrecht; Boston: Kluwer Academic.
Paul EL, Atiemo-Obeng VA, Kresta SM, editors. 2004. Handbook of industrial mixing: Science and practice. Hoboken: John Wiley & Sons.
Perry RH, Green D, editors. 1984. Perry's chemical engineering handbook. Chicago: R.R.Donnelley & Sons Company.
Reuveny S, Kim YJ, Kemp CW, Shiloach J. 1993. Effect of temperature and oxygen on cell growth and recombinant protein production in insect cell cultures. Appl Microbiol Biotechnol 38:619–623.
Schena M, Shalon D, Davis RW, Brown PO. 1995. Quantitative monitoring of gene expression patterns with a complementary DNA microarray. Science 270(20):467–470.
Schopf B, Howaldt MW, Bailey JE. 1990. DNA distribution and respiration activity of *Spodoptera frugiperda* populations infected with wild-type and recombinant *Autographa californica* nuclear polyhedrosis virus. J Biotechnol 15:169–186.
Shuler ML, Kargi F. 2002. Bioprocess engineering: Basic concepts. Upper Saddle River: Prentice Hall PTR.
Shuler ML, Wood HA, Granados RR, Hammer DA, editors. 1995. Baculovirus expression systems and biopesticides. New York; Chichester; Brisbane; Toronto; Singapore: Wiley-Liss.
Stanbury PF, Whitaker A, Hall S. 1995. Principles of fermentation technology. Oxford; Burlington: Elsevier Science.
Szita N, Boccazzi P, Zhang Z, Boyle P, Sinskey AJ, Jensen KF. 2005. Development of a multiplexed microbioreactor system for high-throughput bioprocessing. Lab on a Chip 5(8):819–826.
Taticek RA. 1995. Enhanced recombinant protein expression in baculovirus-infected high-density insect cell suspension cultures and the operation of a continuous flow bioreactor. Ithaca: Cornell University.
Taticek RA, Shuler ML. 1997. Effect of elevated oxygen and glutamine levels on foreign protein production at high cell densities using the insect cell-baculovirus expression system. Biotechnol Bioeng 54:142–152.
Taticek RA, Choi C, Phan S-E, Palomares LA, Shuler ML. 2001. Comparison of growth and recombinant protein expression in two different insect cell lines in attached and suspension culture. Biotechnol Prog 17:676–684.
Tramper J, Williams JB, Joustra D. 1986. Shear sensitivity of insect cells in suspension. Enzyme Microb Technol 8:33–36.
Weiss SA, Orr T, Smith GC, Kalter SS, Vaughn JL, Dougherty EM. 1982. Quantitative measurement of oxygen consumption in insect cell culture infected with polyhedrosis virus. Biotechnol Bioeng 24:1145–1154.
Yates JR III, Speicher S, Griffin PR, Hunkapiller T. 1993. Peptide mass maps: A highly informative approach to protein identification. Anal Biochem 214(2):397–408.
Zanzotto A, Szita N, Boccazzi P, Lessard P, Sinskey AJ, Jensen KF. 2004. Membrane-aerated microbioreactor for high-throughput bioprocessing. Biotechnol Bioeng 87(2):243–254.
Zhang Z, Szita N, Boccazzi P, Sinskey AJ, Jensen KF. 2005. A well-mixed, polymer-based microbioreactor with integrated optical measurement. Biotechnol Bioeng 93(2):286–296.
Zhang Z, Boccazzi P, Choi H-G, Perozziello G, Sinskey AJ, Jensen KF. 2006. Microchemostat—Microbial continuous culture in a polymer-based instrumented microbioreactor. Lab on a Chip 6(7):906–913.